IOSR Journal of Electrical and Electronics Engineering (IOSR-JEEE)
e-ISSN: 2278-1676,p-ISSN: 2320-3331, Volume 11, Issue 1 Ver. I (Jan – Feb. 2016), PP 54-73
www.iosrjournals.org

Enhanced Restoration in a Restructured Power System with Hydrogen Energy Storage and Unified Power Flow Controller

R.Thirunavukarasu[1], I.A.Chidambaram[2]
[1] *Assistant Professor,* [2]*Professor*
Department of Electrical Engineering, Annamalai University, Annamalainagar, Tamilnadu, India, Pin-608002

Abstract : *This paper proposes evaluation of Power System Restoration Indices (PSRI) based on the Automatic Generation Control (AGC) assessment of interconnected power system in a deregulated environment. This paper deals with the procedure involved in the AGC of a two-area reheat power system having a coordinated control action between Hydrogen Energy Storage (HES) unit and Unified Power Flow Controller (UPFC) for controlling the network performance in a very fast manner and to improve the power transfer limits in order to have a better restoration. In addition to that a new Proportional-Double Integral (PI^2) controller is designed and implemented in the AGC loop and the controller parameters are optimized through Bacterial Foraging Optimization (BFO) algorithm. Simulation results reveal that the proposed PI^2 controller ensures good stability during load variations, excellent transient and dynamic responses when compared with the system comprising PI controller. Moreover the AGC loop with HES coordinated with UPFC have greatly improve the dynamic response and it reduces the control input requirements and to ensure not only the improved PSRI but also to provide less the restoration time, thereby improving the system reliability.*

Keywords: *Hydrogen Energy Storage, PI^2 controller, Power System Restoration Indices, Unified Power Flow Controller.*

I. Introduction

The primary objectives of the Automatic Generation Control (AGC) are to balance the total system generation against system load and losses so that the desired frequency and power interchange with neighboring systems are maintained [1]. The deregulated power system consists of Generation companies (Genco), Distribution companies (Disco), Transmission companies (Transco) and Independent System Operator (ISO) with an open assess policy. In the newly emerged structure, all the Gencos may or may not participate in the AGC task. As a matter of fact, the Independent System Operator (ISO) leads the AGC scheme more reliable. Many investigations in the area of AGC problem for the Interconnected Power System in a deregulated environment have been reported over the past six decades [2-7]. These studies try to modify the conventional LFC system to take into account the effect of bilateral contracts on the dynamics and improve the dynamic and transient response of the system under various operating conditions. The frequency and the power exchanges among areas are kept at their desired values using feedback for the integral of the Area Control Error (ACE), containing the frequency deviation and the error of the tie-line power, and or by controlling the generator prime movers. The controllers so designed regulate the ACE to zero.

Several classical controllers such as Integral (I), Proportional-Integral (PI), Integral-Derivative (ID), and Proportional-Integral-Derivative (PID) have been adopted in AGC and their performance are more or less the same from the practical viewpoint of the dynamic responses. However, the Integral-Double Derivative (IDD) controller provides much better response than the aforesaid controllers [8]. But the Double Derivative controller produces saturation effects and also amplifies the noise signals produced in the system. Unlike a pure Proportional controller, a Proportional plus Integral (PI) controller can track the step change and eventually reduce the error to zero. Similarly, there is need for controllers that tracks the ramp type inputs. PI controller produces steady-state offset for a ramp signal similarly to the way a proportional controller does for a step change. Even though PI controller is very simple for implementation and gives a better dynamic response, their performances deteriorate when the complexity in the system increases due to the nature of the disturbances [9]. A controller with two integrators can able to reduce the area control error to zero even the system has complexities [10, 11]. In this study Proportional-Double Integral (PI^2) controllers are designed and implemented in AGC loop for an interconnected restructured power system. The two integral time-constants values of the PI^2 controller which cause repeated roots in the controller transfer function, minimizing any adverse impact on the closed-loop stability as compared with PI controller. The gain values of PI and PI^2 controllers are tuned using Bacterial Foraging Optimization (BFO) algorithm. BFO algorithm is a computational intelligence based optimization technique which exhibits foraging behavior of e.coli bacteria. The BFO has been demonstrated in [12, 13] which mimics the bacteria forage over a landscape of nutrients to perform parallel non

gradient optimization. In this algorithm is not large affected by the size and nonlinearity of the problem and can converge the solution to an optimal solution where most of the analytical methods fail to converge.

Due to the deregulation of the power industry worldwide, and the most revolutionary change in the industry structure, power systems are operated closer and closer to their limits. Furthermore, in recent years, they have grown considerably in size and complexity. This has led to an increasing number of blackouts, such as the large power outage. The main goal in the power system restoration problem is to determine new control configurations with the minimum active power loss to retain the load demand and adopting optimal switching sequence to improve the power quality. Large-scale power system when faces severe disturbance requires quick recovery of the power system [14, 15] and can some what be able to avoid blackouts with the black start units which can be able to produce power for the auxiliaries of the thermal units without black start capabilities [16]. Under this situation a conventional frequency control i.e., a governor may no longer be able to compensate for such load changes due to the slow response. Therefore, in an inter-area mode, damping out the critical electromechanical oscillations is essential and has to be implemented properly in an interconnected system. Proper monitoring of the system frequency deviations and remedial actions to overcome frequency excursions are more likely to protect the system before it enters an emergency mode of operation. Special attention is therefore given to the behavior of network parameters, control equipments as they affect the voltage and frequency regulation during the restoration process. During restoration due to wide fluctuations in the frequency and voltage it becomes very difficult to maintain the integrity in the system. The purpose of this paper is to provide a conceptually computational methodology for ensuring the system restoration strategies in a faster manner. To achieve a faster restoration process, new black start generators or active power source can be installed allowing network reconfigurations and the load recovery can also be adopted in accelerating the system restoration.

Most of the options proposed so far for the AGC have not been fruitfully implemented in practice due to system operational constraints associated with thermal power plants. The instantaneous mismatch between supply and demand of real power for the sudden load changes can be reduced by the addition of active power sources with fast response. Some of the energy storage devices are designed to meet these needs are fly wheels, battery energy storage, compressed air, energy storage, pumped hydro, fuel cells, Superconducting Magnetic Energy Storage (SMES), etc. Most of these technologies when implemented to independently store electrical energy rate face inefficient discharge in addition to their own inherent disadvantages [17]. In order to compensate for sudden load changes, a fast-acting energy storage systems having storage capacity in addition to the kinetic energy of the generator rotors is advisable to damp out the frequency oscillations. Most options proposed so far for LFC have not been implemented due to system operational constraints associated with thermal power plants. The main reason is the non-availability of required power other than the stored energy in the generator rotors, which can improve the performance of the system, in the wake of sudden increased load demands. In order to compensate for sudden load changes, an active power source with fast response such as Hydrogen Energy Storage (HES) has a wide range of applications such as power quality maintenance for decentralized power supplies. The HES systems has effective short-time overload output and have efficient response characteristics in the particular [18, 19]. The HES will have a wide range of applications such as power quality maintenance for deregulated power supplies. However, it will be difficult to locate the placement of HES in every possible area in the interconnected system due to the economical reasons. The recent advances in power electronics have led to the development of the Flexible Alternating Current Transmission System (FACTS) devices as one of the most effective ways to improve power system operation controllability and power transfer limits. The Unified Power Flow Controller (UPFC), the transmitted power can be controlled by changing three parameters namely transmission magnitude voltage, impedance and phase angle. In UPFC is the most promising version of FACTS devices as it serves to control simultaneously all the three parameters especially voltage, impedance and phase angle [20-23]. In this study to develop more effective and fast restoration in the interconnected power system by computing various Power System Restoration Indices (PSRI) for Two Area Thermal Reheat Interconnected Power System (TATRIPS) in a restructured environment without and with HES and UPFC units. From the simulated results it is observed that the restoration process for the TATRIPS with HES and UPFC to ensure improved Power System Restoration Assessment Indices (PSRAI) in order to provide good margin of stability.

II. AGC In Deregulated Environment

The electrical power system is quite complex and dynamic in nature. Transformation from Vertically Integrated Utilities (VIU) to open energy market system is the main concept of restructured environment to enhance the economical efficiency of power system. In the restructured or deregulated environment the power systems consists of Genco, Disco, Transco and ISO. An agreement between Disco and Genco should be established to supply regulation. The LFC in a deregulated electricity market should be designed to consider different types of possible transactions, such as Poolco-based transactions, bilateral-based transactions and

contract violations-based transactions. In the open market based bilateral contracts, Discos have the freedom to contract with any of the Genco in the own area or other area and these contracts are made under supervision of ISO. Same as Discos, ISO will also have freedom to get power from the same or other areas to provide efficient ancillary services to the system. Therefore, in system with an open access policy, there is a need for a LFC model which can be used for analysis as well as for the development of efficient control strategies. To make the visualization of contracts easier, the concept of a "DISCO Participation Matrix" (DPM) will be used [5] which essentially provides the information about the participation of a Disco in contract with a Genco. In DPM, the number of rows has to be equal to the number of Gencos and the number of columns has to be equal to the number of Discos in the system. Any entry of this matrix is a fraction of total load power contracted by a Disco toward a Genco. As a results total of entries of column belong to Disco_i of DPM is $\sum_i cpf_{ij} = 1$. In this study two-area interconnected power system in which each area has two Gencos and two Discos. Let Genco_1, Genco_2, Disco_1, Disco_2 be in area 1 and Genco_3, Genco_4, Disco_3, Disco_4 be in area 2 as shown in Fig 1. The corresponding DPM is given as follows

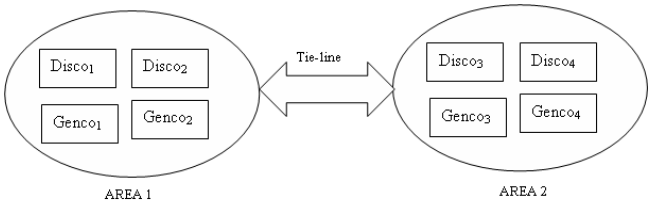

Fig .1 Schematic diagram of two-area system in restructured environment

$$DPM = \begin{bmatrix} & D & I & S & C & O & \\ & cpf_{11} & cpf_{12} & cpf_{13} & cpf_{14} & & E \\ & cpf_{21} & cpf_{22} & cpf_{23} & cpf_{24} & & N \\ & cpf_{31} & cpf_{32} & cpf_{33} & cpf_{34} & & C \\ & cpf_{41} & cpf_{42} & cpf_{43} & cpf_{44} & & O \end{bmatrix} \quad (1)$$

where *cpf* represents "Contract Participation Factor" based on which the Genco has to follow the load demanded by the Disco. The actual and scheduled steady state power flow through the tie-line are given

$$\Delta P_{tie1-2,\,scheduled} = \sum_{i=1}^{2}\sum_{j=3}^{4} cpf_{ij}\,\Delta P_{L\,j} - \sum_{i=3}^{4}\sum_{j=1}^{2} cpf_{ij}\,\Delta P_{L\,j} \quad (2)$$

$$\Delta P_{tie1-2,\,actual} = \left(2\pi T_{12}/s\right)\left(\Delta F_1 - \Delta F_2\right) \quad (3)$$

And at any given time, the tie-line power error $\Delta P_{tie1-2,\,error}$ is defined as

$$\Delta P_{tie1-2,\,error} = \Delta P_{tie1-2,\,actual} - \Delta P_{tie1-2,\,scheduled} \quad (4)$$

The error signal is used to generate the respective ACE signals as in the traditional scenario

$$ACE_1 = \beta_1 \Delta F_1 + \Delta P_{tie\ 1-2,\,error} \quad (5)$$

$$ACE_2 = \beta_2 \Delta F_2 + \Delta P_{tie\ 2-1,\,error} \quad (6)$$

For two area system as shown in Fig.1, the contracted power supplied by i [th] Genco is

$$\Delta Pg_i = \sum_{j=1}^{DISCO=4} cpf_{ij}\,\Delta P_{L\,j} \quad (7)$$

Also note that $\Delta P_{L1,LOC} = \Delta P_{L1} + \Delta P_{L2}$ and $\Delta P_{L2,LOC} = \Delta P_{L3} + \Delta P_{L4}$. In the proposed LFC implementation, the contracted load is fed forward through the DPM matrix to Genco set points. The actual loads affect system dynamics via the input $\Delta P_{L,LOC}$ to the power system blocks. Any mismatch between actual and contracted demands will result in frequency deviations that will drive LFC to re-dispatch the Gencos according to ACE participation factors, i.e., apf_{11}, apf_{12}, apf_{21} and apf_{22}.

III. Design Of Various Controllers

3.1 Design of Proportional-Integral Controller

The conventional Proportional-Integral (PI) controller, Proportional control reduces the peak over-shoot in the damping oscillations of system response and Integral control provides zero state error in frequency

deviation and tie line power flow. In load frequency control nominal parameters of system is achieved with the generation of proper control signal by the PI controller is given by

$$u(t) = K_P \; ACE(t) + \frac{K_P}{T_i} \int ACE(t)\, dt \tag{8}$$

Proportional controller is used to reach the steady state condition much quicker because of the fast transient response with proportional controller. The proportional term of the controller produces a control signal proportional to the Area control Error (ACE) in the system, so that $u(t) = K_P \; ACE(t)$ where K_P is the proportional gain. Typically, given a step change of load demand, low values of K_P give rise to stable responses with large steady-state errors. Higher values of K_P give better steady-state performance, but worse transient response. Therefore, the higher value of K_P is used to reduce the steady state error, although increasing the gain K_P decreases the system time constant and damping. Therefore it is evident to choose the optimum value of K_P. The proportional action can never eliminate the steady state error in the system because some (small) error must be present in order to produce a control output. A common way of reducing the steady state error is by incorporating integral action into the controller. Here, the control signal generated is proportional to the integral of the error signal, that is, where K_I is the integral gain. While an error exists, the integrator tends to increase control action, thus driving the plant output towards the demand output. Then, when the error disappears, the continuing integrator output can be used to maintain the control action necessary for steady-state conditions. But, if the gain of integrator K_I is sufficiently high, overshoot will occur increasing sharply as a function of the gain, this is highly undesirable. Lower value of K_I reduces overshoot but increases rise time of the system. Based upon discussion it is required to design both the K_P and K_I properly.

3.2. Design of Proportional-Double Integral (PI^2) controller

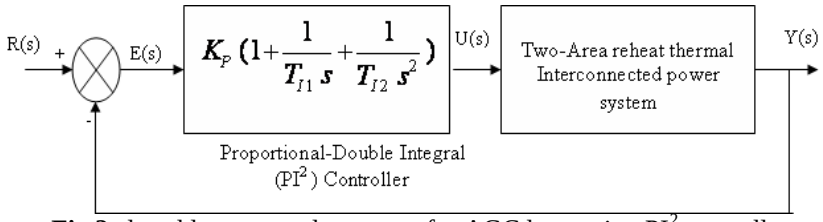

Fig.2 closed loop control structure for AGC loop using PI^2 controller

The ability of proportional integral (PI) controllers to compensate most practical industrial processes has led to their wide acceptance in industrial applications. The ideal continuous time domain PI controller for a single input single output process is expressed in the Laplace domain as follows:

$$G_c(s) = k_P \; (1 + \frac{1}{T_i \; s}) \tag{9}$$

with T_i = integral time constant. If $T_i = \infty$ (i.e. P control), then the closed loop measured value will always be less than the desired value for processes without an integrator term, as a positive error is necessary to keep the measured value constant, and less than the desired value. The introduction of integral action facilitates the achievement of equality between the measured value and the desired value, as a constant error produces an increasing controller output. In PI controller proportional gain provides stability and high frequency response and Integral gain ensures that the average error is driven to zero. However, there are a number of disadvantages to the ultimate cycle tuning approach:(i) the system must generally be destabilized under proportional control, (ii) the empirical nature of the method means that uniform performance is not achieved in general, (iii) several trials must typically be made to determine the ultimate gain, (iv) the resulting process upsets may be detrimental to product quality (v) there is a danger of misinterpreting a limit cycle as representing the stability limit and the amplitude of the process variable signal may be so great that the experiment may not be carried out for cost or safety considerations. So no long term error, as the two gains are tuned. This normally provides high responsive systems. But the predominant weakness of PI controller is it often produces excessive overshoot to a step command. The PI controller lacks a windup function to control the integral value during saturation. So that the Integral gain in PI controller is limited relatively to small values because of the overshoot in the transient response. The disadvantage of adopting integral controller alone is that it tends to make the system unstable because it responds slowly towards the produced error. A controller with two integrators is required to reduce this error to zero. Belanger and Luyben [10] had undertaken an analytical approach for tuning the Proportional-Double Integral (PI^2) controllers and relate the prescribed tuning parameters to the ultimate gain and period of the plant [10]. Simple formulae were used to define the tuning parameters for PI^2 controller and the settings are given by $K_P = 0.33K_u$, $T_{I1} = 2.26\,T_u$, $T_{I2} = 20.5\,T_u^{\,2}$ [11]. This study is based on a numerical

optimization approach rather than an algebraic one, and uses a more general error metric than damping ratio. The effect of the restriction relating the two controller integral time constants can be examined since optimal tunings with and without the restriction can be calculated. Additionally, faster systems can be controlled using this approach since true first order responses are allowed by the chosen model form, in contrast to the more limited type of responses available when the model is restricted to consist of only one integrator. In this study Proportional-Double Integral (PI^2) controllers is used for AGC loop of an interconnected power system as shown in Fig.2. The PI^2 controllers are expressed in Laplace form as follows [10]:

$$G_c(s) = k_P\ (1 + \frac{1}{T_{I1}\ s} + \frac{1}{T_{I2}\ s^2}) \tag{10}$$

In this work optimum gain values are tuned based on Area Control Error of the output response of the system (especially the frequency deviation and tie-line power deviation) and with these gain values the performance of the system is analyzed. And here in this case study it is used as a feedback controller which drives the plant to be controlled within a weighted sum of error and integral of that value i.e. it produces an output signal consisting of three terms one proportional to error signal and the other proportional to integral of error signal. In order to satisfy the above requirements, PI^2 controller gains in the LFC loop are to be optimized using BFO algorithm. In the present work Integral Square Error (ISE) criterion [24] is used to minimize the objective function [J]. The objective function is minimized using Bacterial Foraging Optimization Technique and are represented as follows.

$$\begin{aligned} U_1 &= -K_p\ ACE_1\ - K_{I1}\int ACE_1\ dt - K_{I2}\int ACE_1\ dt \\ U_2 &= -K_p\ ACE_{21}\ - K_{I1}\int ACE_2\ dt - K_{I2}\int ACE_2\ dt \end{aligned} \tag{11}$$

The relative simplicity of this controller is a successful approach towards the zero steady state error in the frequency of the system.

IV. Application Of HES And UPFC Units For AGC In Deregulated Environment Design Of Various Controllers

4.1 Hydrogen Energy Storage System (HESS

Generally the optimization of the schedule of distributed energy sources depends on the constraints of the problem which are load limits, actual generation capabilities, status of the battery, forecasted production schedule. Hydrogen is a serious contender for future energy storage due to its versatility. Consequently, producing hydrogen from renewable resources using electrolysis is currently the most desirable objective available.

4.1.1 Aqua Electrolyzer for production of Hydrogen

An aqua electrolyzer is a device that produces hydrogen and oxygen from water. Water electrolysis is a reverse process of electrochemical reaction that takes place in a fuel cell. An aqua electrolyzer converts dc electrical energy into chemical energy stored in hydrogen. From electrical circuit point of view, an aqua electrolyzer can be considered as a voltage-sensitive nonlinear dc load. For a given aqua electrolyzer, within its rating range, the higher the dc voltage applied, the larger is the load current. That is, by applying a higher dc voltage, more H_2 can be generated. In this paper, the aqua electrolyzer is considered as a subsystem which absorbs the rapidly fluctuating output power. It generates hydrogen and stores in the hydrogen tank and this hydrogen is used as fuel for the fuel cell.

4.1.2 Constant electrolyzer power

The effects of operating the electrolyzer at constant power has to be studied which is the common practice for conventional electrolysis plants. The electrolyzer and the hydrogen storage tanks are designed so that no wind energy is dissipated, and the amount of hydrogen obtained is more efficient. The electrolyzer rating is decided to be equal to [18]

$$P_e^{\max} = p_w^{\max} - P_g^{\max} - \min\left(P_i\ (t)\right) \tag{12}$$

The hydrogen storage tanks are sized according to the following criterion [18].

$$0 < V_H(t) - V_H^{\max} \qquad for \quad t = 1....N \tag{13}$$

So that the hydrogen storage does not reach the lower and upper limits during the simulation period. For each of the hydrogen-load scenarios, simulations have been run for different wind power capacities. The required hydrogen storage capacity for the different hydrogen-filling scenarios and wind power capacities have to be obtained which results in a nonlinear relationship between the required hydrogen storage and the installed wind power. It can be noted that for a fixed wind power capacity, a lower hydrogen-filling rate leads to larger hydrogen storage as with the normal operating conditions; only excess wind power is used for hydrogen

production. If the hydrogen-filling rate is low, it takes longer time to reduce the hydrogen content in the storage tanks. Thus, a higher storage capacity is necessary to prevent that the upper limit is reached. The production cost of hydrogen as a function of wind power capacity for the different hydrogen-filling scenarios. The hydrogen production cost increases rapidly, because of the extra investment in electrolyzer and especially hydrogen storage tanks needed to prevent dissipation of wind energy. All the curves of hydrogen filling scenarios reach a point where the increase in cost changes significantly. This point is chosen as the maximum preferable wind power capacity for the corresponding scenario. Hydrogen production cost increases approximately linearly with wind power capacity below this point. A part of P_{WPG} or/and P_{PV} is to be utilized by AE for the production of hydrogen to be used in fuel-cell for generation of power. The transfer function can be expressed as first order lag:

$$G_{AE}(s) = \frac{K_{AE}}{1+sT_{AE}} \tag{14}$$

Fuel cell for energy storage

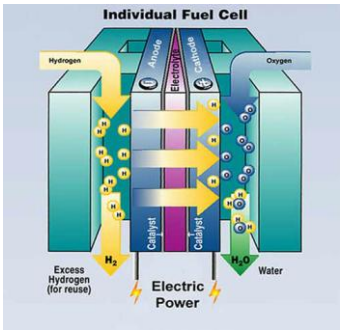

Fig 3 Structure of a fuel cell

Fuel cells are static energy conversion device which converts the chemical energy of fuel (hydrogen) directly into electrical energy. They are considered to be an important resource in hybrid distributed power system due to the advantages like high efficiency, low pollution etc. An electrolyzer uses electrolysis to breakdown water into hydrogen and oxygen. The oxygen is dissipated into the atmosphere and the hydrogen is stored so it can be used for future generation. A fuel cell converts stored chemical energy, in this case hydrogen, directly into electrical energy. A fuel cell consists of two electrodes that are separated by an electrolyte as shown in Fig 3. Hydrogen is passed over the anode (negative) and oxygen is passed over the cathode (positive), causing hydrogen ions and electrons to form at the anode. The energy produced by the various types of cells depends on the operation temperature, the type of fuel cell, and the catalyst used. Fuel cells do not produce any pollutants and have no moving parts. The transfer function of Fuel Cell (FC) can be given by a simple linear equation as

$$G_{FC}(s) = \frac{K_{FC}}{1+sT_{FC}} \tag{15}$$

Hydrogen is one of the promising alternatives that can be used as an energy carrier. The universality of hydrogen implies that it can replace other fuels for stationary generating units for power generation in various industries. Having all the advantages of fossil fuels, hydrogen is free of harmful emissions when used with dosed amount of oxygen, thus reducing the greenhouse effect [19]. Essential elements of a hydrogen energy storage system comprise an electrolyzer unit which converts electrical energy input into hydrogen by decomposing water molecules, the hydrogen storage system itself and a hydrogen energy conversion system which converts the stored chemical energy in the hydrogen back to electrical energy as shown in Fig 4. The over all transfer function of hydrogen Energy storage unit has can be

$$G_{HES}(s) = \frac{K_{HES}}{1+sT_{HES}} = \frac{K_{AE}}{1+sT_{AE}} * \frac{K_{FC}}{1+sT_{FC}} \tag{16}$$

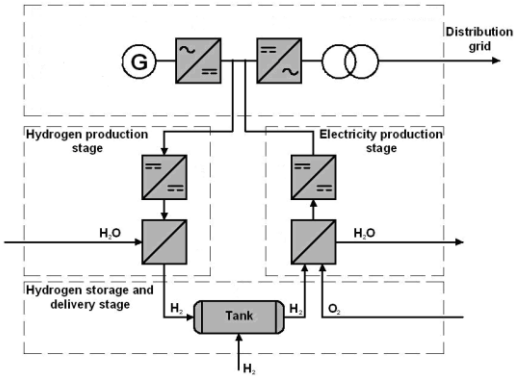

Fig 4 Block diagram of the hydrogen storage unit

4.2 Mathematical Model of UPFC unit

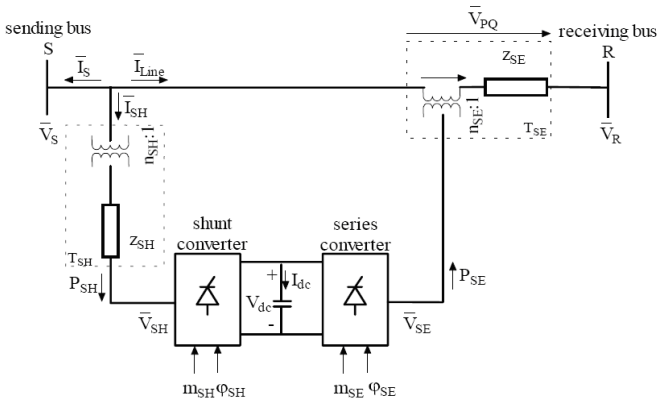

Fig.5 Fundamental frequency model of UPFC

The UPFC is a device placed between two busses referred to as the UPFC sending bus and the UPFC receiving bus. It consists of two Voltage-Sourced Converters (VSCs) with a common DC link. For the fundamental frequency model, the VSCs are replaced by two controlled voltage sources as shown in Fig.5 [23]. The voltage source at the sending bus is connected in shunt and will therefore be called the shunt voltage source. The second source, the series voltage source, is placed between the sending and the receiving busses. The UPFC is placed on high-voltage transmission lines. This arrangement requires step-down transformers in order to allow the use of power electronics devices for the UPFC. Applying the Pulse Width Modulation (PWM) technique to the two VSCs the following equations for magnitudes of shunt and series injected voltages are obtained

$$V_{SH} = m_{SH} \frac{V_{DC}}{2\sqrt{2}n_{SH}V_B} \tag{17}$$

$$V_{SE} = m_{SE} \frac{V_{DC}}{2\sqrt{2}n_{SE}V_B} \tag{18}$$

Where: m_{SH} – Amplitude modulation index of the shunt VSC control signal, m_{SE} – Amplitude modulation index of the series VSC control signal, n_{SH} – shunt transformer turn ratio, n_{SE} – Series transformer turn ratio, V_B – The system side base voltage in kV, V_{DC} – DC link voltage in kV. The phase angles of V_{SH} and V_{SE} are

$$\delta_{SH} = \angle(\delta_S - \varphi_{SH})$$
$$\delta_{SE} = \angle(\delta_S - \varphi_{SE}) \tag{19}$$

Where φ_{SH} is the firing angle of the shunt VSC with respect to the phase angle of the sending bus voltage, φ_{SE} is the firing angle of the series VSC with respect to the phase angle of the sending end bus Voltage. The series converter injects an AC voltage $V_{SH} = V_{SE}\angle(\delta_S - \varphi_{SE})$ in series with the transmission

line. Series voltage magnitude V_{SE} and its phase angle φ_{SE} with respect to the sending bus which is controllable in the range of $0 \leq V_{SE} \leq V_{SE\,\max}$ and $0 \leq \varphi_{SE} \leq 360^0$.

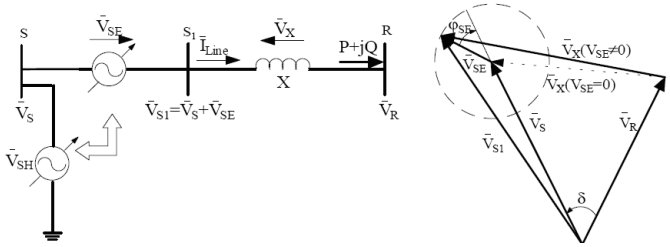

Fig 6. Application of UPFC in the tie-line

The shunt converter injects controllable shunt voltage such that the real component of the current in the shunt branch balance the real power demanded by the series converter. The real power can flow freely in either direction between the AC terminals. On the other hand as the reactive power cannot flow through the DC link, it is being absorbed or generated locally by each converter. The shunt converter operated to exchange the reactive power with the AC system provides the possibility of independent shunt compensation for the line. If the shunt injected voltage is regulated to produce a shunt reactive current component that will keep the sending end bus voltage at its pre-specified value, then the shunt converter is operated in the Automatic Voltage Control Mode. Shunt converter can also be operated in the Var Control Mode. In this case shunt reactive current is produced to meet the desired inductive or capacitive Var requirement. UPFC is placed in the transmission line connecting buses S and R as shown in Fig 6 [23]. Line conductance was neglected. UPFC is represented by two ideal voltage sources of controllable magnitude and phase angle. Bus S and fictitious bus S_1 are shown in Fig 6 which represents UPFC' s sending and receiving buses respectively. In this case, the complex power received at the receiving end of the line is given by

$$S = \overline{V_R}\ \overline{I}_{Line}^{\,*} = \overline{V}_R \left(\frac{\overline{V}_S + \overline{V}_{SE} - \overline{V}_R}{jX} \right)^* \tag{20}$$

Where $\overline{V_{SE}} = V_{SE} \angle(\delta_S - \varphi_{SE})$

The complex conjugate of this complex power is

$$S^* = P - jQ = \overline{V_R}^* \left(\frac{\overline{V_S} + \overline{V}_{SE} - \overline{V_R}}{jX} \right) \tag{21}$$

Performing simple mathematical manipulations and separating real and imaginary components of (21) the following expressions for real and the reactive powers received at the receiving end of the line are

$$P = \frac{V_S V_R}{X} \sin\delta + \frac{V_R V_{SE}}{X} \sin(\delta - \varphi_{SE}) = P_O(\delta) + P_{SE}(\delta, \varphi_{SE})$$
$$Q = -\frac{V_R^{\,2}}{X} + \frac{V_S V_R}{X} \cos\delta + \frac{V_R V_{SE}}{X} \cos(\delta - \varphi_{SE}) = Q_O(\delta) + Q_{SE}(\delta, \varphi_{SE}) \tag{22}$$

For $V_{SE} = 0$ the above equations represent the real and reactive powers of the uncompensated system. As the UPFC series voltage magnitude can be controlled between 0 and V_{SE} max, and its phase angle can be controlled between 0 and 360 degrees at any power angle, and using in (22) the real and reactive power received at bus R for the system with the UPFC unit is installed can be controlled between rotation of the series injected voltage phasor with RMS value of V_{SEmax} from 0 to 360^0 allows the real and the reactive power flow to be controlled within the boundary

$$P_{\min}(\delta) \leq P \leq P_{\max}(\delta)$$
$$Q_{\min}(\delta) \leq Q \leq Q_{\max}(\delta) \tag{23}$$

V. System Modelling For Control Design

The HES and UPFC units are found to be superior to the governor system in terms of the response speed against, the frequency fluctuations. Therefore, the operational tasks are assigned according to the response speed as follow. The HES and UPFC units are charged with suppressing the peak value of frequency deviations quickly against the sudden load change, subsequently the governor system acts for compensating the steady state error of the frequency deviations. Fig 7 shows the model for the control design of HES and UPFC units. Where the dynamics of governor systems are eliminated by setting the mechanical inputs to be constant since

the response of governor is much slower than that of HES or UPFC units. Then the state equation of the system represented by Fig 7 becomes

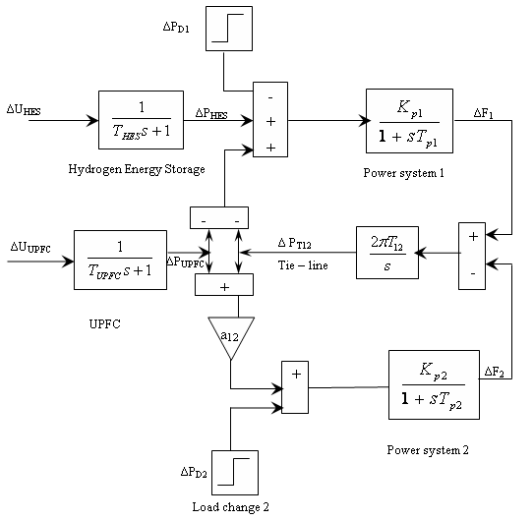

Fig. 7 Linearized reduction model for the control design

$$\begin{bmatrix} \Delta\dot{F}_1 \\ \Delta\dot{P}_{T12} \\ \Delta\dot{F}_2 \end{bmatrix} = \begin{bmatrix} -\frac{1}{T_{p1}} & -\frac{k_{p1}}{T_{p1}} & 0 \\ 2\pi T_{12} & 0 & -2\pi T_{12} \\ 0 & \frac{a_{12}\, k_{p2}}{T_{p2}} & -\frac{1}{T_{p2}} \end{bmatrix} \begin{bmatrix} \Delta F_1 \\ \Delta P_{T12} \\ \Delta F_2 \end{bmatrix} + \begin{bmatrix} \frac{k_{p1}}{T_{p1}} & -\frac{k_{p1}}{T_{p1}} \\ 0 & 0 \\ 0 & \frac{a_{12}\, k_{p2}}{T_{p2}} \end{bmatrix} \begin{bmatrix} \Delta P_{HES} \\ \Delta P_{UPFC} \end{bmatrix} \tag{24}$$

Here, from the physical view point it is noted that the UPFC located between two areas is effective to stabilize the inter-area oscillation mode only, and then the HES which is capable of supplying the energy into the power system can be utilized for the control of the inertia mode.

5.1 Control design of Hydrogen Energy Storage unit

The design process starts from the reduction of two area system into one area which represents the Inertia centre mode of the overall system. The controller of HES is designed in the equivalent one area system to reduce the frequency deviation of inertia centre. The equivalent system is derived by assuming the synchronizing coefficient T_{12} to be large. From the state equation of $\Delta\dot{P}_{T12}$ in (24)

$$\frac{\Delta\dot{P}_{T12}}{2\pi T_{12}} = \Delta F_1 - \Delta F_2 \tag{25}$$

Setting the value of T_{12} in (25) to be infinity yields $\Delta F_1 = \Delta F_2$. Next, by multiplying state equation of $\Delta\dot{F}_1$ *and* $\Delta\dot{F}_2$ in (24) by $\frac{T_{p1}}{k_{p1}}$ and $\frac{T_{p2}}{a_{12}\, k_{p2}}$ respectively, then

$$\frac{T_{p1}}{k_{p1}}\Delta\dot{F}_1 = -\frac{1}{k_{p1}}\Delta F_1 - \Delta P_{T12} - \Delta P_{UPFC} + \Delta P_{HES} \tag{26}$$

$$\frac{T_{p2}}{a_{12}\, k_{p2}}\Delta\dot{F}_2 = \frac{-1}{k_{p2}\, a_{12}}\Delta F_2 + \Delta P_{T12} + \Delta P_{UPFC} \tag{27}$$

By summing (26) and (27) and using the above relation $\Delta F_1 = \Delta F_2 = \Delta F$

$$\Delta\dot{F} = \frac{\left(-\frac{1}{k_{p1}} - \frac{1}{k_{p2}a_{12}}\right)}{\left(\frac{T_{p1}}{k_{p1}} + \frac{T_{p2}}{k_{p2}a_{12}}\right)}\Delta F + \frac{1}{\left(\frac{T_{p1}}{k_{p1}} + \frac{T_{p2}}{k_{p2}a_{12}}\right)}\Delta P_{HES} + C\Delta P_D \tag{28}$$

Where the load change in this system ΔP_D is additionally considered, here the control $\Delta P_{RFB} = -K_{HES}\,\Delta F$ is applied then.

$$\Delta F = \frac{C}{s + A + K_{HES}\ B}\ \Delta P_D \tag{29}$$

Where $A = \left(-\frac{1}{k_{p1}} - \frac{1}{k_{p2}a_{12}} \right) \Big/ \left(\frac{T_{p1}}{k_{p1}} + \frac{T_{p2}}{k_{p2}a_{12}} \right); B = \frac{1}{\left[\frac{T_{p1}}{K_{p1}} + \frac{T_{p2}}{K_{p2}a_{12}} \right]}$

Where C = proportionality constant between change in frequency and change in load demand. Since the control purpose of HES is to suppress the deviation of ΔF quickly against the sudden change of $\Delta P_{D,}$ the percent reduction of the final value after applying a step change ΔP_D can be given as a control specification. In (29) the final values with K_{HES} = 0 and with $K_{HES} \neq 0$ are C/A and C/(A+K_{HES} B) respectively therefore the percentage reduction is represented by

$$C/(A + K_{HES}\ B) \Big/ (C/A) = R/100 \tag{30}$$

For a given R, the control gain of HES unit is calculated as

$$K_{HES} = \frac{A}{BR}(100 - R) \tag{31}$$

5.2 Control design of Unified Power Flow Controller unit

The controller for the UPFC is design to enhance the damping of the inter-area mode. In order to extract the inter-area mode from the system in (24), the concept of overlapping decompositions is applied. First, the state variables of the system (24) are classified into three groups, i.e. $x_1 = [\Delta F_1], x_2 = [\Delta P_{T12}], x_3 = [\Delta F_2].$ next, the system (24) is decomposed into two decoupled subsystems. Where the state variable ΔP_{T12} is duplicated included in both subsystems, which is the reason that this process is called overlapping decompositions. Then, one subsystem which preserves the inter-area mode is represented by.

$$\begin{bmatrix} \Delta \dot{F}_1 \\ \Delta \dot{P}_{T12} \end{bmatrix} = \begin{bmatrix} -\frac{1}{T_{p1}} & \frac{-Kp_1}{T_{p1}} \\ 2\pi T_{12} & 0 \end{bmatrix} \begin{bmatrix} \Delta F_1 \\ \Delta P_{T12} \end{bmatrix} + \begin{bmatrix} \frac{-Kp_1}{T_{p1}} \\ 0 \end{bmatrix} [\Delta P_{UPFC}] \tag{32}$$

It has been proved that the stability of original system is guaranteed by stabilizing every subsystem. Therefore the control scheme of UPFC is designed to enhance the stability of the system (32) by eigenvalue assignment method. Here let the conjugate eigenvalue pair of the system (32) be α ± jβ, which corresponds to the inter-area mode. The control purpose of the UPFC is to damp the peak value of frequency deviation in area 1 after a sudden change in the load demand. Since the system (32) is the second order oscillation system, the percentage overshoot *Mp (new)* can be specified for the control design. *Mp (new)* is given as a function of the damping ratio by

$$M_{p(new)} = e^{(-\pi\delta/\sqrt{1-\delta^2})} \tag{33}$$

The real and imaginary parts of eigenvalue after the control are expressed by

$$\alpha_s = \delta\,\omega_n \tag{34}$$

$$\beta_s = \omega_n \sqrt{1-\delta^2} \tag{35}$$

Where w_n is the undamped natural frequency, by specifying *Mp* and assuming $\beta_s = \beta$, the desired pair of eigenvalue is fixed. As a result, the eigenvalue assignment method derives to feed back scheme as

$$\Delta P_{UPFC} = -k_1 \Delta F_1 - k_2 \Delta P_{T12} \tag{36}$$

The characteristic polynomial of the system (32) with state feedback, which is given by

$$|\lambda I - (A - BK)| = 0 \tag{37}$$

Where state feedback gain matrix $K = [k_1, k_2]$. The desired characteristic polynomial from the specified eigenvalue (μ_1, μ_2) is given by

$$(\lambda - \mu_1)(\lambda - \mu_2) = 0 \tag{38}$$

By equating the coefficients of (37) and (38) the elements k_1, k_2 of state feedback gain matrix K are obtained.

5.3 Structure of UPFC-based damping controller

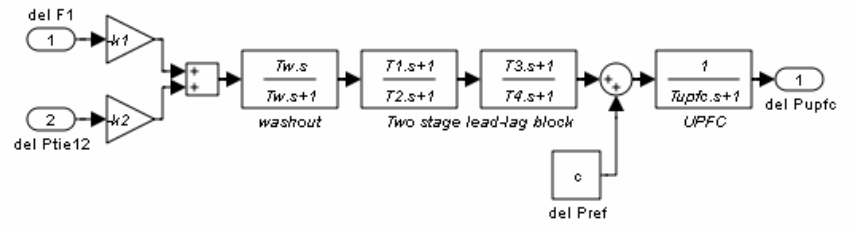

Fig.8 Structure of UPFC-based damping controller

The active power controller of UPFC has a structure of Lead-Lag compensator with output signal ΔP_{ref}. In this study the dynamic characteristics of UPFC is modeled as the first order controller with time constant T_{upfc} . It is to be noted that the injected power deviations of UPFC, ΔP_{upfc} acting positively for area 1 and reacts negatively for area 2. Therefore ΔP_{upfc} flow into both of the areas with different signs (+,-) simultaneously. The commonly used Lead-Lag structure is chosen in this study as UPFC based supplementary damping controller as shown in Fig 8. The structures consist of a gain block, a washout block and two-stage phase compensation block. The phase compensation block provides the appropriate phase-lead characteristics to compensate for the phase lag between input and output signals. The input signals associated with oscillations is passed unchanged would modify the output. The input signal of the proposed UPFC-based controller is frequency deviations Δf and tie- line power deviations and the output is the change in control vector ΔP_{upfc} . From the washout function point of view the value of washout time constant is not critical in Lead-Lag structured controllers and can have a range between 1 to 20 seconds. Thus, there are five parameters such as the time constants T_{upfc}, T_1, T_2, T_3 and T_4 to be optimized using BFO algorithms for the optimal design for stabilizing the frequency.

VI. Power System Restoration

Power system restoration is well recognized as an important task to reduce the duration of a disturbance that occurs in power systems. The high level strategy of the system restoration plan is to restore the integrity of the interconnection as quickly as possible. Power system disturbances are most likely to occur as the result of loss of generating units, transmission facilities, or as the result of unexpected load changes. These disturbances may be affecting the reliable operation of the power system. The associated conditions under severe system disturbances generally result in critically loaded transmission facilities, critical frequency deviations, or high or low voltage conditions. Each Transmission / Generation owner has an obligation to protect their own system's equipment and reliability. However, the steps taken to do so be achieved with the coordinated control action with the System Operator so as to solve the problem in a best manner [25, 26]. In general, the following steps are taken by ISO, Transmission Owners and Generation Operators: (i) Perform a system assessment to determine extent of outage, (ii) Start Black Start units to form islands, (iii) Build cranking paths to other generating units (iv) Restore critical load Synchronize and interconnect islands to form larger islands, (v) Connect to outside areas and Return to normal operations. The system restoration strategies are found closely related to the systems' characteristics. After analyzing the system conditions and characteristics of outages, system restoration planners or dispatchers will select the Power System Restoration Indices (PSRI) which were obtained based on system dynamic performances and the remedial measures to be taken can be adjudged. In this study two-area interconnected reheat thermal in a restructured environment without and with HES and UPFC units are considered. More over Power System Restoration Indices namely Feasible Restoration Indices (FRI) when the system is operating in a normal condition with Gencos units in operation and Comprehensive Restoration Indices (CRI) are one or more Gencos unit outage in any area. From these Restoration Indices the restorative measures like the magnitude of control input, rate of change of control input required can be adjudged. The Feasible Restoration Indices are calculated as follows

The Feasible Restoration Indices 1 (ε_1) is obtained as the ratio between the settling time of frequency deviation in area 1 (ς_{s1}) and power system time constant (T_{p1}) of area 1

$$\varepsilon_1 = \frac{\varsigma_{s1}}{T_{p1}} \tag{39}$$

The Feasible Restoration Indices 2 (ε_2) is obtained as the ratio between the settling time of frequency deviation in area 2 (ς_{s2}) and power system time constant (T_{p2}) of area 2

$$\varepsilon_2 = \frac{\varsigma_{s2}}{T_{p2}} \tag{40}$$

The Feasible Restoration Indices 3 (ε_3) is obtained as the ratio between the settling time of Tie –line power deviation (ς_{s3}) and synchronous power coefficient T_{12}

$$\varepsilon_3 = \frac{\varsigma_{s3}}{T_{12}} \tag{41}$$

The Feasible Restoration Indices 4 (ε_4) is obtained as the peak value frequency deviation $\Delta F_1(\varsigma_p)$ response of area 1 exceeds the final value $\Delta F1(\varsigma_s)$

$$\varepsilon_4 = \Delta F_1(\varsigma_p) - \Delta F_1(\varsigma_s) \tag{42}$$

The Feasible Restoration Indices 5 (ε_5) is obtained as the peak value frequency deviation $\Delta F_2\ (\varsigma_p)$ response of area 2 exceeds the final value $\Delta F2\,(\varsigma_s)$

$$\varepsilon_5 = \Delta F_2(\varsigma_p) - \Delta F_2(\varsigma_s) \tag{43}$$

The Feasible Restoration Indices 6 (ε_6) is obtained as the peak value tie-line power deviation $\Delta P_{tie}\ (\varsigma_p)$ response exceeds the final value $\Delta P_{tie}\ (\varsigma_s)$

$$\varepsilon_6 = \Delta P_{tie}(\varsigma_p) - \Delta P_{tie}(\varsigma_s) \tag{44}$$

The Feasible Restoration Indices 7 (ε_7) is obtained from the peak value of the control input deviation $\Delta P_{c1}(\varsigma_p)$ response of area 1 with respect to the final value $\Delta P_{c1}(\varsigma_s)$

$$\varepsilon_7 = \Delta P_{c1}(\varsigma_p) - \Delta P_{c1}\ (\varsigma_s) \tag{45}$$

The Feasible Restoration Indices 8 (ε_8) is obtained from the peak value of the control input deviation $\Delta P_{c2}(\varsigma_p)$ response of area 2 with respect to the final value $\Delta P_{c2}(\varsigma_s)$

$$\varepsilon_8 = \Delta P_{c2}(\varsigma_p) - \Delta P_{c2}\ (\varsigma_s) \tag{46}$$

Apart from the normal operating condition of the test system few other case studies like one unit outage in any area, outage of one distributed generation in both areas are considered individually. The optimal controller gains and their performance of the system various case studies the corresponding the Comprehensive Restoration Indices (CRI) ($\varepsilon_9, \varepsilon_{10}, \varepsilon_{11}, \varepsilon_{12}, \varepsilon_{13}, \varepsilon_{14}, \varepsilon_{15}, \varepsilon_{16}$) is obtained from (39- 46).

VII. Simulation Results And Observations

In this test system all the Gencos in each area consists of thermal reheat units with different capacity and the active power model of HES is places in area 1 and UPFC unit located in series with the tie-line is shown in Fig.9. The nominal parameters are given in Appendix [27]. The proposed controllers are designed and implemented in Two-Area Thermal Reheat Interconnected Power System (TATRIPS) without and with HES and UPFC units for different types of transactions. The optimal solution of control inputs is taken an optimization problem, and the cost function in (8) and (11) is derived using the frequency deviations of control areas and tie- line power changes. The gain value of HES (K_{HES}) is calculated using in (31) for the given value of speed regulation coefficient (R). The purpose of utilizing UPFC unit is to damp out the peak value of frequency deviations in the both areas and tie-line power deviations. Since the system in (31) is second order oscillations system, the peak over shoot *Mp (new)* can be specified in Table 1 and corresponding feed back gains K_1 and K_2 are found using Eq (36). The control parameters of HES and TCPS are shown in the Table 1. Then PI controller gain values ($K_{Pi}\ K_{I\,i,}$) and PI^2 controller gain values ($K_{Pi}, K_{I1i,}\ K_{I\,2i}$) for each area and parameters of UPFC unit ($T_{UPFC,}$ T_1, T_2, T_3 and T_4) are optimized are tuned simultaneously with help of BFO algorithm for both traditional and bilateral based LFC schemes in TATRIPS with a wide range of load changes for different case studies. The results are obtained by MATLAB 7.01 software and 50 iterations are chosen for the convergence of the solution in the BFO algorithm. The optimum PI and PI^2 controller gain values for a TATRIPS are tuned for various case studies and are tabulated in the Tables 2 and 3 respectively and the damping controller parameters value of UPFC unit is T_{UPFC} = 0.018, T_1= 0.525, T_2 = 0.611, T_3 = 0.984, and T_4 = 0.127. From the Table 4, and 5, it can be observed that the proposed PI^2 controller show better performance and convergence than that of the PI controller for different case studies. The stability analysis yields easy and

direct control gain tuning guidelines, which guarantee asymptotic convergence of the close loop system. Moreover the values of PSRI are found to be improved a lot.

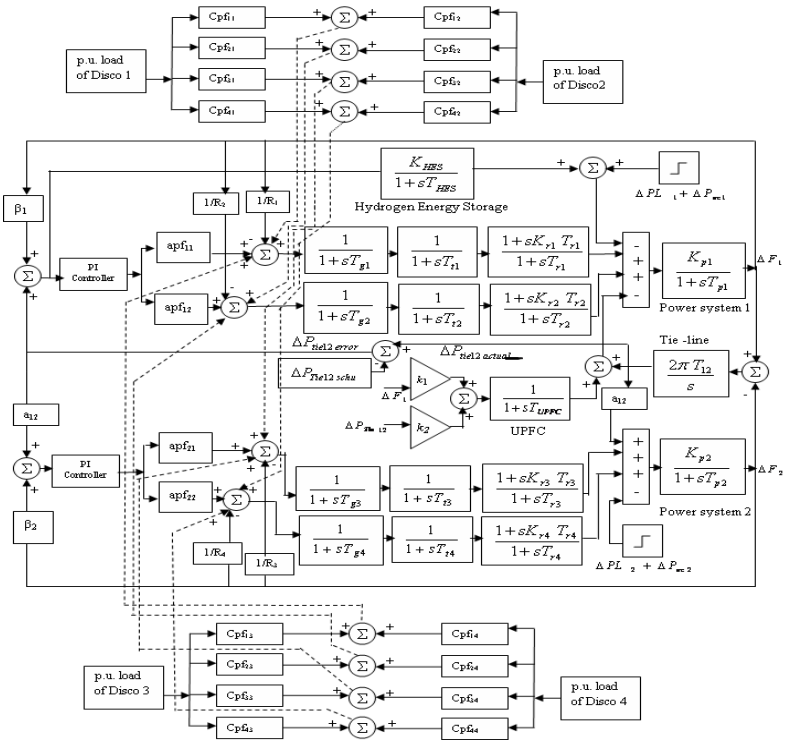

Fig. 9 Linearized model of a two-area Thermal reheat interconnected power system in a restructured environment with HES and UPFC unit

7.1 Feasible Restoration Indices

7.7.1: Poolco based transaction

In this scenario, Gencos participate only in the load following control of their areas. It is assumed that a large step load 0.1 pu MW is demanded by each Disco in area 1. Assume that a case of Poolco based contracts between Dicos and available Gencos is simulated based on the following Disco Participation Matrix (DPM) referring to Eq (1) is considered as

$$DPM = \begin{bmatrix} 0.5 & 0.5 & 0 & 0 \\ 0.5 & 0.5 & 0 & 0 \\ 0 & 0 & 0 & 0 \\ 0 & 0 & 0 & 0 \end{bmatrix} \tag{47}$$

$Disco_1$ and $Disco_2$ demand identically from their local Gencos, viz., $Genco_1$ and $Genco_2$. Therefore, $cpf_{11} = cpf_{12} = 0.5$ and $cpf_{21} = cpf_{22} = 0.5$. It may happen that a Disco violates a contract by demanding more power than that specified in the contract and this excess power is not contracted to any of the Gencos. This uncontracted power must be supplied by the Gencos in the same area to the Disco. It is represented as a local load of the area but not as the contract demand. Consider scenario-1 again with a modification that Disco demands as given in Table 2 and 3. From the simulation results Power System Restoration Indices namely Feasible Restoration Indices are evaluated using in (39)-(46) from dynamic output responses of the proposed test system TATRIPS without HES/ UPFC using either PI or PI^2 controller is shown in Table 4 and 5 respectively and test system TATRIPS with HES and UPFC using PI^2 controller is shown in Table 6 (case 1- 4).

7.1.2: Bilateral transaction

Here all the Discos have contract with the Gencos and the following Disco Participation Matrix (DPM) be considered.

$$DPM = \begin{bmatrix} 0.5 & 0.25 & 0.5 & 0.4 \\ 0.2 & 0.25 & 0.2 & 0.2 \\ 0.0 & 0.3 & 0.2 & 0.25 \\ 0.3 & 0.2 & 0.1 & 0.15 \end{bmatrix} \tag{48}$$

In this case, the $Disco_1$, $Disco_2$, $Disco_3$ and $Disco_4$, demands 0.15 pu.MW, 0.05 pu.MW, 0.15 pu.MW and 0.05 pu.MW from Gencos as defined by cpf in the DPM matrix and each Gencos participates in LFC as defined by the following ACE participation factor $apf_{11} = apf_{12} = 0.5$ and $apf_{21} = apf_{22} = 0.5$. The comparative transient performances of two-area Power System with HES and UPFC using PI^2 controller for given load perturbation as shown in Fig 10 and it can observed that the oscillations in the area frequencies and tie-line power deviation have decreased to a considerable extent as compare to that of the system without HES and UPFC units. The corresponding Feasible Restoration Indices are calculated from dynamic output responses of the proposed test system TATRIPS without HES and UPFC using either PI or PI^2 controller is shown in Table 4 and 5 respectively and test system TATRIPS with HES and UPFC using PI^2 controller is shown in Table 6 (case 5- 8).

7.2 Comprehensive Restoration Indices

Apart from the normal operating condition of the test systems few other case studies like outage generating unit in any area and uncontracted power demand in any area during outage the corresponding Power System Restoration Indices is called Comprehensive Restoration Indices (CRI). In this study Genco-4 in area 2 is outage and uncontracted power demand in any area and Disco Participation Matrix (48) is considered. The comparative transient performances of two-area Power System without and with HES and UPFC unit using PI^2 controller for given load perturbation and corresponding Comprehensive Restoration Indices (CRI) are calculated and tabulated in Table 7, 8 and 9. From the simulated results it is observed that the restoration process of the system with HES and UPFC unit ensures not only reliable operation but provides a good margin of stability compared without HES and UPFC.

7.3 Power System Restoration Assessment

Power System Restoration Indices (PSRI) based on the Automatic Generation Control (AGC) assessment of interconnected power can be used in different ways: (i) Automatic power system restoration. (ii) Operator support, suggesting actions to the operator in real time. (iii) Off-line planning for restoration in advance of the blackout. This includes both comparing different restoration plans/strategies' and comparing restoration sequences after modifications in the net. The main focus in this paper PSRI are useful for system planners for restoration planning in advance.

(i) If $1.0 \leq \varepsilon_1, \varepsilon_2, \varepsilon_9, \varepsilon_{10} \leq 5$ and $40 \leq \varepsilon_3, \varepsilon_{11} \leq 50$, then the system subject to a large steady error for step load changes. Under a steady state condition, change in frequency of each area and change in tie-line power exchange will become more in some of case studies in Table 4-6. The integral control action are required based on the performance criteria such as ACE must be equal to zero at least one time in all 10-minute periods and average deviation of ACE from zero must be within specified limits based on a percentage of system generation for all 10-minutes periods. So that the above case studies, the integral controller gain (K_I) is made very large then only steady state frequency error reduces to zero. In other words, this means that speed regulation (R) should be made equal to zero, which is not desirable. Proportional control is not suitable for reducing the steady state error to zero. So that integral controller gain of each control area has to be increased causing the speed changer valve to open up widely. Thus the speed- changer position attains a constant value only when the frequency error is reduced to zero. A PI^2 controller implemented in this study for AGC loop to reduce steady state error to zero for step and ramp type set points and it requires lesser control effort in order to improve the PSRI as compared to PI controller.

(ii) If $\varepsilon_1, \varepsilon_2, \varepsilon_9, \varepsilon_{10} \geq 5$ and $\varepsilon_3, \varepsilon_{11} \geq 50$ then the system required more amount of distributed generation requirement is needed and the FACTS devices are needed to improvement tie-line power oscillations. In this cases, the gain of the integrator is sufficiently high, over shoot will occur, increasing sharply as a function of the gain; this is highly undesirable. In the absence of integral control, one can sharply increase the gain of the closed- loop system and thereby improves the system response. However, the system will have a steady- state error. So that a TATRIPS coordinated with HES and UPFC unit for LFC application has improve relatively stability of the power system.

(iii) If $0.5 \leq \varepsilon_4, \varepsilon_5, \varepsilon_{12}, \varepsilon_{13} \leq 1$ and $0.15 \leq \varepsilon_7, \varepsilon_8, \varepsilon_{15}, \varepsilon_{16} \leq 0.2$ then the system required the stabilization of frequency oscillations in an interconnected power system. The conventional load-frequency controller may no longer be able to attenuate the large frequency oscillation due to the slow response of the governor for unpredictable load variations. So that in deregulated system, regulation and load following are the two frequency-related ancillary services required for balancing the varying load with matching generation. Ancillary Services are defined as all those activities on the interconnected grid that are necessary to support the transmission of active power while maintaining reliable operation and ensuring the required degree of quality and security. These ancillary services are priced separately and ISO has to purchase these services from the ancillary service providers and

distribute to the consumers. In a deregulated environment, any power system controls such as the LFC as an ancillary service acquires a principal role to maintain the electric system reliability at an adequate level and is becoming much more significant today in accordance with the complexity of interconnected power system. In this study a fast-acting energy storage system such as HES having storage capacity in addition to the kinetic energy of the generator rotors is advisable to damp out the frequency oscillations.

(iv) If $0.05 \leq \varepsilon_6, \varepsilon_{14} \leq 0.15$ then the FACTS devices are needed to improvement tie-line power oscillations. The recent advances in power electronics have led to the development of the Flexible Alternating Current Transmission Systems (FACTS). As these FACTS devices are capable of controlling the network condition in a very fast manner the usage of FACTS devices are more apt to improve the stability of power system. In this study UPFC is one of the FACTS devices that can change the relative phase angle between the system voltages therefore, the real power flow can be regulated to mitigate the frequency oscillations and enhance power system stability.

If $\varepsilon_4, \varepsilon_5, \varepsilon_{12}, \varepsilon_{13} \geq 1$, $\varepsilon_6, \varepsilon_{14} \geq 0.15$ and $\varepsilon_7, \varepsilon_8, \varepsilon_{15}, \varepsilon_{16} \geq 0.2$ then the system is vulnerable and the system becomes unstable and may result to blackout. Small blackouts, involving only a few substations, can often be handled rather easily since they occur more often than the larger blackouts so the operators has more experience with them and the load can often be reconnected as soon as the operational reserves are able to meet the demand. Larger blackouts, affecting the whole or significant parts of the power system, are much harder to restore since large parts of the power system need to be energized and a significant part of the generating units will not be available. In order to handle restoration situations the operators have prepared restoration plans and guidelines for some typical blackout situations. The operators have to adopt these to the current situation. Two major strategies in power system restoration can be defined, bottom up vs. top down. Bottom up means that several smaller electrical islands are started in parallel; these are then used to energize the transmission system. The need to synchronize the islands can slow down the process. Top down means that the transmission system is energized from one point and all the lower voltage levels are energized from the transmission system and the whole energized power system is kept synchronized

VIII. Conclusion

This paper proposes the design procedure for obtaining Power System Restoration Assessment Indices (PSRI) which indicates the requirements to be adopted in minimizing the frequency deviations, tie-line power deviation of a two-area interconnected restructured power system to ensure the reliable operation of the power system. In these PSRI can be utilized to help system operators in real time by suggesting relevant actions taken to adhere for the automation of the power system restoration. Traditional PI and the proposed PI^2 controllers are designed using BFO algorithm and implemented in a restructured power system. The proposed PI^2 controllers, represents a version of the classical PI controller, where an extra feedback signal and Integral term is added. The effectiveness of the proposed PI^2 controller is tested in a two-area deregulated power system for a wide range of load demands and disturbances under different operating conditions. The proposed PI^2 controller shows better performance to ensure improved PSRI in order to provide reduce the restoration time, thereby improving the system reliability than PI controller. BFO Algorithm is found to be easy to implement without additional computational complexity, with quite promising results and ability to jump out the local optima. Moreover the dynamic output responses of first peak frequency deviation of both areas and tie-line power oscillations following sudden load disturbances in either of the areas can be suppressed a controlling the phase angle of UPFC unit. Then HES unit contributes a lot in promoting the efficiency of the overall generation control through load leveling and the assurance of LFC capacity after overload characteristic and quick responsiveness. It may be concluded that the design concept of damping out the inertia mode and inter-area mode, the coordinated control with HES and UPFC units are found to be more effective to suppress the frequency deviations of the two area system. From the simulated results it is also observed that the restoration process for the Thermal generating unit with HES and UPFC units are more sophisticated control for a better restoration of the power system output responses and to ensure improved PSRAI in order to provide good margin of stability.

Acknowledgement

The authors wish to thank the authorities of Annamalai University, Annamalainagar, Tamilnadu, India for the facilities provided to prepare this paper.

Table 1 Results obtained based on the control design with HES and UPFC units

1	Gain value of HES unit (31) K_{HES} = 0.902
2	Eigenvalue of system without UPFC (32) λ1 = - 0.25 +j 1.8081 λ2 = - 0.25 – j 1.8081
3	Inter-area mode, without UPFC Mp = 64.85%
4	Design specification, with UPFC Mp(new) =5 %
5	New Eigenvalue of the system with UPFC (32) λ1(new) = -1.724 + j1.8081 λ2(new) = -1.724 - j1.8081
6	State Feed back Gain value of UPFC (36) [K_1,K_2]= [-0.566, -0.908]

Table 2 Optimized Controller parameters of the TATRIPS using PI controller for the corresponding Load demand change

TATRIPS	PI controller gain of Area 1		PI controller gain of Area 2		Load demand in pu.MW				un contracted load demand pu.MW	
	K_P	K_I	K_P	K_I	$Disco_1$	$Disco_2$	$Disco_3$	$Disco_4$	Area1	Area 2
Case 1	0.341	0.459	0.191	0.081	0.1	0.1	0.0	0.0	0.0	0.0
Case 2	0.384	0.315	0.121	0.051	0.1	0.1	0.0	0.0	0.1	0.0
Case 3	0.411	0.489	0.284	0.112	0.1	0.1	0.0	0.0	0.0	0.1
Case 4	0.386	0.352	0.256	0.127	0.1	0.1	0.0	0.0	0.1	0.1
Case 5	0.316	0.512	0.127	0.296	0.15	0.05	0.15	0.05	0.0	0.0
Case 6	0.393	0.575	0.131	0.305	0.15	0.05	0.15	0.05	0.1	0.0
Case 7	0.324	0.492	0.214	0.362	0.15	0.05	0.15	0.05	0.0	0.1
Case 8	0.381	0.563	0.249	0.368	0.15	0.05	0.15	0.05	0.1	0.1
Case 9	0.421	0.685	0.247	0.183	0.12	0.08	0.14	0.06	0.0	0.0
Case 10	0.438	0.696	0.255	0.178	0.12	0.08	0.14	0.06	0.1	0.0
Case 11	0.416	0.671	0.252	0.172	0.12	0.08	0.14	0.06	0.0	0.1
Case 12	0.435	0.678	0.261	0.186	0.12	0.08	0.14	0.06	0.1	0.1

Table 3 Optimized Controller parameters of the TATRIPS using PI^2 controller for the corresponding Load demand change

TATRIPS	PI^2 controller gain of Area 1			PI^2 controller gain of Area 2			Load demand in pu.MW				un contracted load demand pu.MW	
	K_P	K_{I1}	K_{I2}	K_P	K_{I1}	K_{I2}	$Disco_1$	$Disco_2$	$Disco_3$	$Disco_4$	Area 1	Area 2
Case 1	0.113	0.067	1.12×10^{-2}	0.063	0.012	5.51×10^{-4}	0.1	0.1	0.0	0.0	0.0	0.0
Case 2	0.127	0.046	4.16×10^{-3}	0.039	0.007	3.47×10^{-4}	0.1	0.1	0.0	0.0	0.1	0.0
Case 3	0.136	0.071	9.35×10^{-3}	0.094	0.016	7.12×10^{-4}	0.1	0.1	0.0	0.0	0.0	0.1
Case 4	0.127	0.052	5.17×10^{-3}	0.085	0.018	1.02×10^{-3}	0.1	0.1	0.0	0.0	0.1	0.1
Case 5	0.104	0.075	1.33×10^{-2}	0.041	0.043	1.11×10^{-2}	0.15	0.05	0.15	0.05	0.0	0.0
Case 6	0.129	0.085	1.35×10^{-2}	0.043	0.044	1.14×10^{-2}	0.15	0.05	0.15	0.05	0.1	0.0
Case 7	0.107	0.072	1.21×10^{-2}	0.071	0.053	9.86×10^{-3}	0.15	0.05	0.15	0.05	0.0	0.1
Case 8	0.126	0.082	1.34×10^{-2}	0.082	0.054	8.76×10^{-3}	0.15	0.05	0.15	0.05	0.1	0.1
Case 9	0.139	0.101	1.79×10^{-2}	0.082	0.027	2.18×10^{-3}	0.12	0.08	0.14	0.06	0.0	0.0
Case 10	0.144	0.102	1.78×10^{-2}	0.084	0.026	2.01×10^{-3}	0.12	0.08	0.14	0.06	0.1	0.0
Case 11	0.137	0.098	1.75×10^{-2}	0.083	0.025	1.89×10^{-3}	0.12	0.08	0.14	0.06	0.0	0.1
Case 12	0.143	0.086	1.71×10^{-2}	0.086	0.027	2.13×10^{-3}	0.12	0.08	0.14	0.06	0.1	0.1

Table 4 FRI for TATRIPS using PI controller for different types of case studies

TATRIPS	FRI based on Settling time (ζ_s)			FRI based on Peak over/ under shoot (m_p)			FRI based on control input deviation (ΔP_c)	
	ε_1	ε_2	ε_3	ε_4	ε_5	ε_6	ε_7	ε_8
Case 1	0.871	0.861	42.63	0.351	0.316	0.042	0.149	0.113
Case 2	0.936	0.875	43.54	0.562	0.402	0.053	0.234	0.124
Case 3	0.901	0.943	46.23	0.432	0.459	0.062	0.143	0.252
Case 4	1.212	1.375	53.63	0.624	0.716	0.081	0.225	0.236
Case 5	0.923	0.896	40.78	0.357	0.456	0.072	0.153	0.093
Case 6	0.949	0.912	41.96	0.553	0.513	0.076	0.264	0.146
Case 7	0.931	0.986	45.51	0.381	0.653	0.081	0.159	0.162
Case 8	1.245	1.312	52.29	0.633	0.991	0.085	0.258	0.178

Table 5 FRI for TATRIPS using PI^2 controller for different types of case studies

TATRIPS	FRI based on Settling time (ζ_s)			FRI based on Peak over/ under shoot (m_p)			FRI based on control input deviation (ΔP_c)	
	ε_1	ε_2	ε_3	ε_4	ε_5	ε_6	ε_7	ε_8
Case 1	0.853	0.837	40.12	0.336	0.294	0.033	0.126	0.096
Case 2	0.915	0.851	41.88	0.541	0.382	0.046	0.213	0.106
Case 3	0.881	0.927	44.91	0.413	0.438	0.051	0.126	0.231
Case 4	1.192	1.332	51.42	0.596	0.702	0.073	0.208	0.219
Case 5	0.901	0.871	38.24	0.309	0.396	0.058	0.113	0.053
Case 6	0.923	0.892	39.73	0.524	0.453	0.061	0.223	0.105
Case 7	0.914	0.961	42.22	0.367	0.618	0.067	0.124	0.119
Case 8	1.224	1.294	50.74	0.608	0.949	0.069	0.213	0.136

Table 6 FRI for TATRIPS with HES and UPFC unit using PI^2 controller for different types of case studies

TATRIPS	FRI based on Settling time (ζ_s)			FRI based on Peak over/ under shoot (m_p)			FRI based on control input deviation (ΔP_c)	
	ε_1	ε_2	ε_3	ε_4	ε_5	ε_6	ε_7	ε_8
Case 1	0.568	0.653	20.57	0.183	0.217	0.012	0.046	0.068
Case 2	0.635	0.665	23.28	0.391	0.311	0.016	0.153	0.085
Case 3	0.591	0.689	24.63	0.317	0.369	0.021	0.076	0.198
Case 4	0.723	0.989	31.58	0.441	0.638	0.043	0.152	0.185
Case 5	0.579	0.697	19.36	0.098	0.212	0.028	0.045	0.031
Case 6	0.621	0.766	22.25	0.308	0.352	0.041	0.166	0.081
Case 7	0.662	0.831	24.97	0.168	0.474	0.043	0.073	0.009
Case 8	0.851	0.993	30.09	0.402	0.725	0.048	0.152	0.102

Table 7 CRI for TATRIPS using PI controller with different types of case studies

TATRIRPS	CRI based on Settling time (ζ_s)			CRI based on Peak over / under shoot (M_p)			CRI based on control input deviation (ΔP_c)	
	ε_9	ε_{10}	ε_{11}	ε_{12}	ε_{13}	ε_{14}	ε_{15}	ε_{16}
Case 9	1.431	1.537	55.48	0.678	0.719	0.156	0.185	0.161
Case 10	1.715	1.678	56.39	0.691	0.701	0.167	0.193	0.167
Case 11	1.525	1.823	59.36	0.705	0.929	0.168	0.187	0.173
Case 12	1.747	1.867	59.29	1.317	1.252	0.173	0.218	0.186

Table 8 CRI for TATRIPS using PI^2 controller with different types of case studies

TATRIRPS	CRI based on Settling time (ζ_s)			CRI based on Peak over / under shoot (M_p)			CRI based on control input deviation (ΔP_c)	
	ε_9	ε_{10}	ε_{11}	ε_{12}	ε_{13}	ε_{14}	ε_{15}	ε_{16}
Case 9	1.386	1.456	54.96	0.503	0.514	0.131	0.182	0.159
Case 10	1.702	1.598	55.13	0.559	0.611	0.148	0.191	0.165
Case 11	1.511	1.736	58.54	0.573	0.836	0.151	0.183	0.169
Case 12	1.716	1.771	58.87	1.185	1.122	0.167	0.215	0.184

Table 9 CRI for TATRIPS with HES and UPFC unit using PI^2 controller with different types of case studies

TATRIRPS	CRI based on Settling time (ς_s)			CRI based on Peak over / under shoot (M_p)			CRI based on control input deviation (ΔP_c)	
	ε_9	ε_{10}	ε_{11}	ε_{12}	ε_{13}	ε_{14}	ε_{15}	ε_{16}
Case 9	0.891	1.224	44.75	0.224	0.238	0.091	0.091	0.119
Case 10	1.114	1.275	45.14	0.238	0.351	0.101	0.101	0.128
Case 11	0.998	1.488	47.36	0.375	0.468	0.112	0.105	0.142
Case 12	1.197	1.597	49.85	1.001	1.003	0.129	0.116	0.151

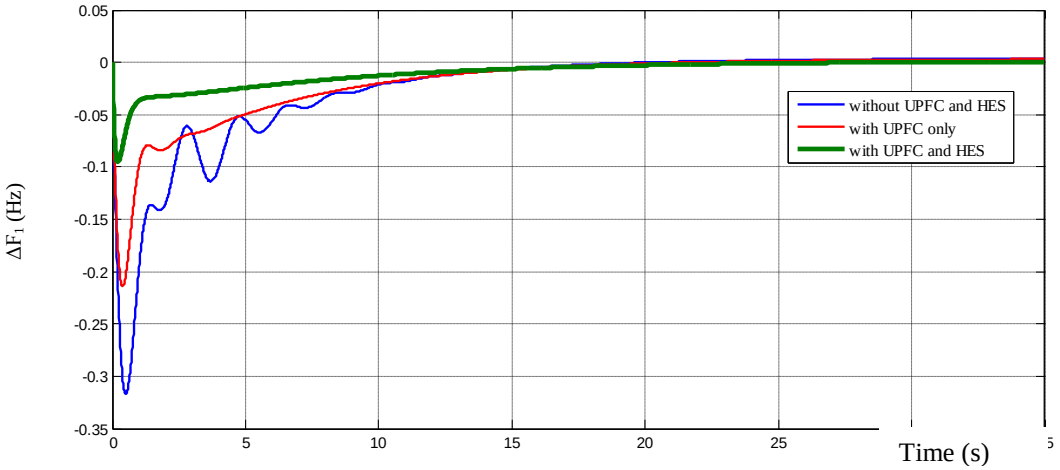

Fig. 10(a) ΔF_1 (Hz) Vs Time (s)

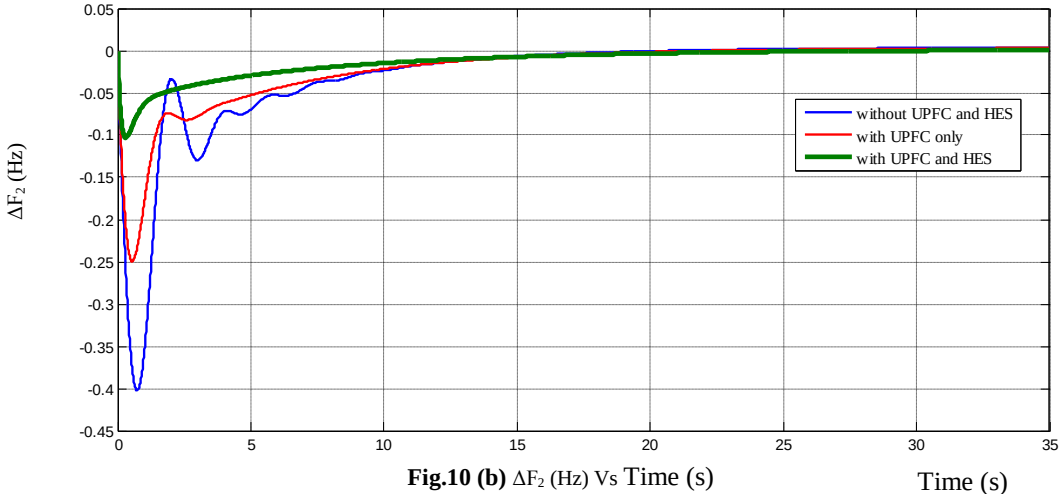

Fig.10 (b) ΔF_2 (Hz) Vs Time (s)

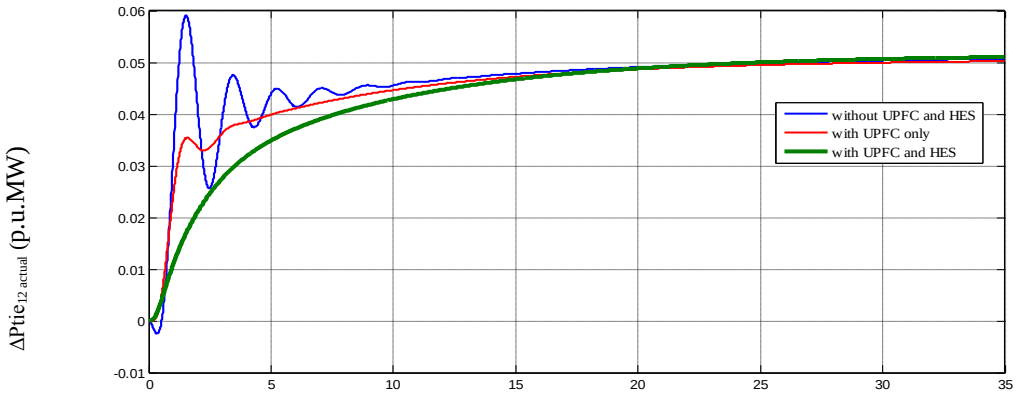

Fig.10 (c) $\Delta Ptie_{12,\ actual}$ (p.u.MW) Vs Time (s)

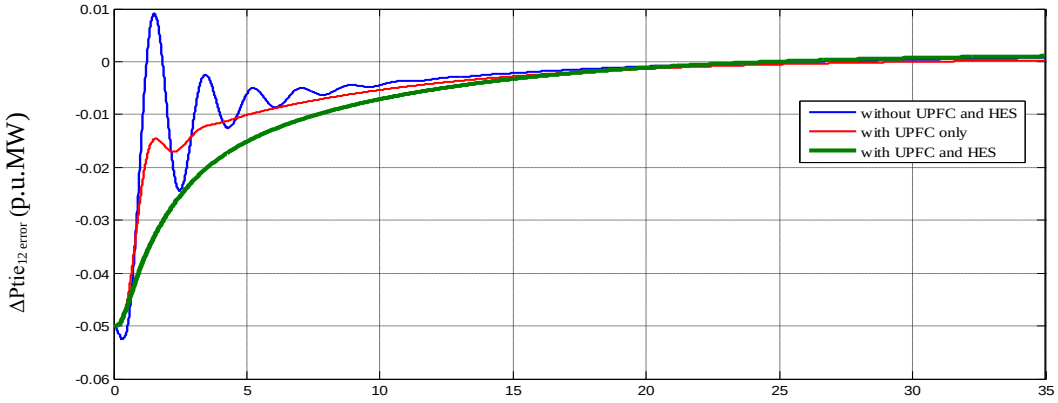

Fig.10(d) $\Delta Ptie_{12,\ error}$ (p.u.MW) Vs Time (s)

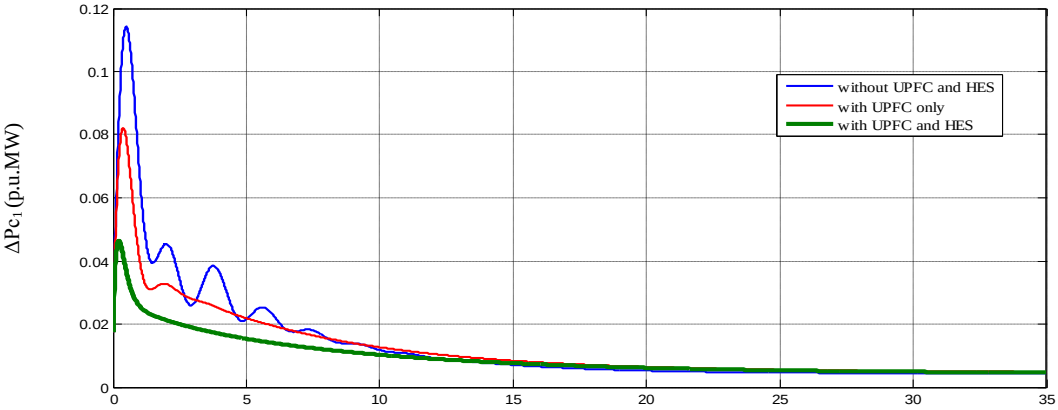

Fig.10 (e) ΔPc_1 (p.u.MW) Vs Time (s)

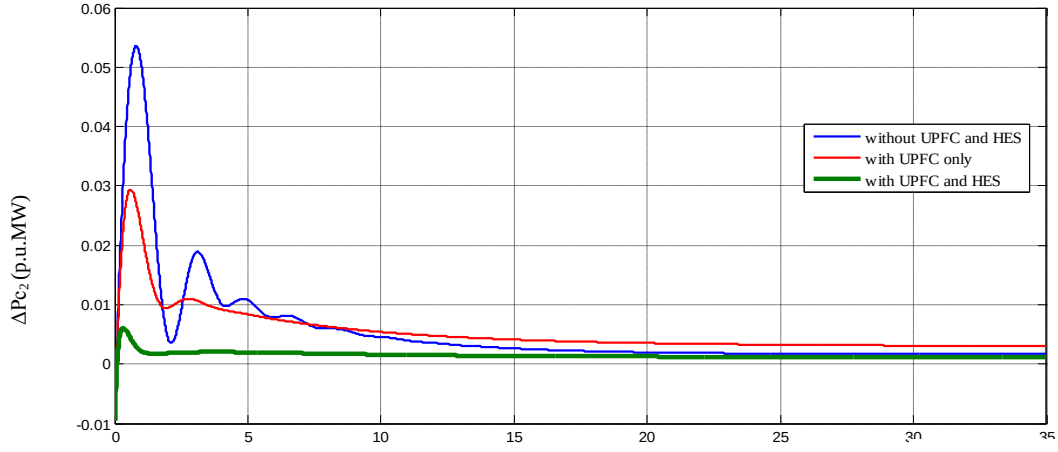

Fig.10 (f) ΔPc_2 (p.u.MW) Vs Time (s)

Fig.10 Dynamic responses of the frequency deviations, tie- line power deviations, and Control input deviations for a two area LFC system without and with HES and UPFC unit using PI^2 controllers in the restructured scenario-2 bilateral based transactions.

References

[1] Mukta, Balwinder Singh Surjan, Load Frequency Control of Interconnected Power System in Deregulated Environment: A Literature Review, International Journal of Engineering and Advanced Technology 2(3) (2013) 435-441

[2] B.Delfino, F.Fornari, S.Massucco, Load-frequency control and inadvertent interchange evaluation in restructured power systems, IEE Proceedings-Generation Transmission and Distribution 149(5) (2002) 607-614.

[3] A.P.Fathima, M.A.Khan, Design of a new market structure and robust controller for the frequency regulation services in the deregulated power system, Electrical Power Components and Systems 36(8) (2008) 864-883.

[4] H. Bevrani, Y. Mitani, K. Tsuji, Robust decentralized LFC in a restructured power system, Energy Conversion and Management, 45 (2004) 2297-2312.

[5] V. Donde, M. A. Pai, I. A. Hiskens, Simulation and optimization in an AGC system after deregulation, IEEE Transactions on Power Systems 16 (3) (2001) 481-489.

[6] L. S. Rao, N.V. Ramana, Recent Philosophies of AGC of a Hydro-thermal System in Deregulated Environment, International Journal of Advances in Engineering and Technology 2(1) (2012) 282-288.
[7] Shaik Farook, P. Sangmeswara Raju, Decentralized Fractional Order PID Controller for AGC in a Multi Area Deregulated Power System, International Journal of Advances in Electrical and Electronics Engineering 1(3) (2013) 317-333.
[8] Lalit Chandra Saikia, J. Nanda, S. Mishra, Performance comparison of several classical controllers in AGC for multi-area interconnected thermal system, Electrical Power and Energy Systems 33 (2011) 394-401.
[9] J.Nanda A.Mangla, S.Suri, Some new findings on automatic generation control of an interconnected hydrothermal system with conventional controllers, IEEE Transactions on Energy Conversion 21 (2006) 187-194.
[10] P. Belanger, W. Luyben, Design of low-frequency compensator for improvement of plant wide regulatory performance, Industrial Engineering Chemistry Research 36 (1997) 5339-5347.
[11] R. Monroy-Loperena, I. Cervantes, A. Morales, J. Alvarez-Ramirez, Robustness and parameterization of the proportional plus double-integral compensator, Industrial Engineering Chemistry Research 38 (1997) 2013-2021.
[12] K.M.Passino, Biomimicry of bacterial foraging for distributed optimization and control, IEEE Control System Magazine 22 (3) (2002) 52-67.
[13] Janardan Nanda, S. Mishra, Lalit Chandra Saikia, Maiden Application of Bacterial Foraging-Based optimization technique in multi-area Automatic Generation Control, IEEE Transactions on Power Systems 24(2) (2009) 602-609.
[14] M.M.Adibi, J.N. Borkoski, R.J.Kafka, T.L. Volkmann, Frequency Response of Prime Movers during Restoration, IEEE Transactions on Power Systems, 14 (2) (1999) 751-756.
[15] M.M.Adibi, R.J.Kafka, Power System Restoration Issues, IEEE Computer Applications in Power 4 (2) (1991) 19-24.
[16] J. Hu, Z. Z. Guo, Y. C. Liu, Q. Y. Guo, Power System Restoration and Analysis Of Restoration Sequence of Generating Sets, Power System Technology 28 (18) (2004) 1-4.
[17] Shashi Kant Pandey, Soumya R. Mohanty, Nand Kishor, A literature survey on load–frequency control for conventional and distribution generation power systems, Renewable and Sustainable Energy Reviews 25 (2013) 318–334.
[18] Dimitris Ipsakis, Spyros Voutetakis, Panos Seferlisa, Fotis Stergiopoulos and Costas Elmasides, "Power management strategies for a stand-alone power system using renewable energy sources and hydrogen storage", International Journal of Hydrogen Energy Vol.34, pp 7081-7095, 2009.
[19] Ke´louwani S, Agbossou K, Chahine R, "Model for energy conversion in renewable energy system with hydrogen storage", Journal of Power Sources, 140 (2005) 392–399.
[20] L. Musirin, .N.Dianah, M.Radzi, M. Murtadha Othman, M.Khayat Idris, T. Khawa Abdul Rahman, Voltage Profile Improvement Using Unified Power Flow Controller via Artificial Immune System, WSEAS Transactions on Power System 3(4) (2008) 49-58.
[21] Muwaffaq I. Alomoush, Derivation of UPFC dc load flow model with examples of its use in restructured power systems**,** IEEE Transactions on Power Systems 18 (2003) 1173-1180.
[22] A.Kazemi, M.R. Shadmesgaran, Extended Supplementary Controller of UPFC to Improve Damping Inter-Area Oscillations Considering Inertia Coefficient, International Journal on Energy 2(1) (2008) 432-440.
[23] E. Uzunovic, C.A.Canizares, J.Reeve, Fundamental Frequency Model of Unified Power Flow Controller, North American Power Symposium, NAPS, Cleveland, Ohio, October 1998, pp.23-28.
[24] Ogata Katsuhiko, Modern Control Engineering, Prentice Hall of India Private Limited, New Delhi, India, 2010.
[25] Q. Liu, L. B. Shi, M. Zhou, G. Y. Li, Y. X. Ni, Optimal Strategy for Units Start-up During Power System Restoration, Transactions of China Electro technical Society 24 (3) (2009) 164-170.
[26] Jun Chen, Wei -xing Zhao, Hua-ying Su, Jia-lin Bai, Nian Liu, Xiao-yan Qiu and Qian Liao, Research on Optimization for Units Start during Power System Restoration, Energy and Power Engineering, 5 (2013) 708-712.
[27] A. Jalili, H. Shayeghi, N.M. Tabatabaei, Fuzzy PID controller base on LFC in the deregulated power system including SMES, International Journal on Technical and Physical Problems of Engineering, 3(3) (2011) 38-47.

APPENDIX

A1. Control Area parameter [27]

A2 Gencos Parameter (Thermal generating unit) [27]

Parameters	Area 1	Area 2
Kp (Hz/p.u.MW)	120	72
Tp (sec)	20	14.3
β (p.u.MW / Hz)	0.8675	0.785
T_{12} (p.u.MW / Hz)	0.545	
a_{12}	-1	

MVA_{Base} (1000 MW) Parameters	Gencos (k in area i)			
	1-1	1-2	2-1	2-2
Rate (MW)	1000	1100	800	900
Tg (sec)	0.06	0.06	0.07	0.08
Tt (sec)	0.36	0.44	0.42	0.4
Tr (sec)	10	10	10	10
Kr	0.5	0.5	0.5	0.5
R (Hz / p.u.MW)	2.4	2.5	3.3	2.4